

See discussions, stats, and author profiles for this publication at: <https://www.researchgate.net/publication/6863641>

Carbon Nanotube Amplification Strategies for Highly Sensitive Immunodetection of Cancer Biomarkers

ARTICLE *in* JOURNAL OF THE AMERICAN CHEMICAL SOCIETY · SEPTEMBER 2006

Impact Factor: 12.11 · DOI: 10.1021/ja062117e · Source: PubMed

CITATIONS

411

READS

45

11 AUTHORS, INCLUDING:



Bernard S Munge

Salve Regina University

21 PUBLICATIONS 1,158 CITATIONS

SEE PROFILE



Ashwinkumar Bhirde

NCI/FDA

33 PUBLICATIONS 1,526 CITATIONS

SEE PROFILE



J. Silvio Gutkind

University of California, San Diego

506 PUBLICATIONS 32,843 CITATIONS

SEE PROFILE



James Francis Rusling

University of Connecticut

217 PUBLICATIONS 9,514 CITATIONS

SEE PROFILE

Published in final edited form as:

J Am Chem Soc. 2006 August 30; 128(34): 11199–11205.

Carbon Nanotube Amplification Strategies for Highly Sensitive Immunodetection of Cancer Biomarkers

Xin Yu[†], Bernard Munge^{†,‡}, Vyomesh Patel[§], Gary Jensen[†], Ashwin Bhird[†], Joseph D. Gong[†], Sang N. Kim[⊥], John Gillespie^{||}, J. Silvio Gutkind[§], Fotios Papadimitrakopoulos^{†,⊥}, and James F. Rusling^{†,‡,⊥}

Contribution from the Department of Chemistry, 55 N. Eagleville Rd., University of Connecticut, Storrs, Connecticut 06269, Department of Pharmacology, University of Connecticut Health Center, Farmington, Connecticut 06032, Department of Chemistry, Salve Regina University, Newport, Rhode Island 02840, Oral and Pharyngeal Cancer Branch, National Institute of Dental and Craniofacial Research, National Institutes of Health, Bethesda, Maryland 20892, Institute of Material Science, University of Connecticut, Storrs, Connecticut 06269, and Pathogenetics Unit, Advanced Technology Center, Laboratory of Pathology and Urologic Oncology Branch, Center for Cancer Research, National Cancer Institute, Bethesda, Maryland 20892–4605 E-mail: james.rusling@uconn.edu

[†] Department of Chemistry, University of Connecticut.

[‡] Department of Pharmacology, University of Connecticut Health Center.

[§] Department of Chemistry, Salve Regina University.

[§] National Institute of Dental and Craniofacial Research, NIH.

[⊥] Institute of Material Science, University of Connecticut.

^{||} Center for Cancer Research, National Cancer Institute, NIH.

Abstract

We describe herein the combination of electrochemical immunosensors using single-wall carbon nanotube (SWNT) forest platforms with multi-label secondary antibody-nanotube bioconjugates for highly sensitive detection of a cancer biomarker in serum and tissue lysates. Greatly amplified sensitivity was attained by using bioconjugates featuring horseradish peroxidase (HRP) labels and secondary antibodies (Ab₂) linked to carbon nanotubes (CNT) at high HRP/Ab₂ ratio. This approach provided a detection limit of 4 pg mL⁻¹ (100 amol mL⁻¹), for prostate specific antigen (PSA) in 10 μL of undiluted calf serum, a mass detection limit of 40 fg. Accurate detection of PSA in human serum samples was demonstrated by comparison to standard ELISA assays. PSA was quantitatively measured in prostate tissue samples for which PSA could not be differentiated by the gold standard immunohistochemical staining method. These easily fabricated SWNT immunosensors show excellent promise for clinical screening of cancer biomarkers and point-of-care diagnostics.

Introduction

Sensitive measurement of proteins is a critical need in many aspects of modern biochemical and biomedical research. Specific applications of protein detection include medical diagnostics, elucidation of disease vectors, immunology, new drug development, proteomics and systems biology.^{1,2} Recent progress in genomics and proteomics has demonstrated the potential of new bioanalytical technology to contribute significantly to disease diagnosis.^{3,4} In particular, clinical measurement of collections of cancer biomarkers shows great promise for highly reliable predictions for early cancer detection.⁵⁻⁹

Point-of-care protein biomarker screening for early cancer detection will require low cost techniques to rapidly measure proteins with high selectivity and sensitivity, while maintaining minimum sample amount and operational simplicity. Modern commercial immunoassays, including the Abbott IMX,¹⁰ Hybritech Tandem E and R,¹¹ Roche Elecsys,¹² and optimized ELISA¹³ achieve detection limits from 10 to 100 pg mL⁻¹ for many proteins in serum, but require 50–150 μ L of serum. While this amount of sample is not too demanding for serum, it poses a significant challenge for analysis of tissues. Proof of concept for new, sensitive protein detection technologies utilizing surface plasmon resonance,^{14,15} nanoparticles,^{16,17} or microcantilevers¹⁸ has been reported. Nano-transistors made from nanotubes or nanowires spanning a gap between two metal contacts^{19–21} have shown excellent sensitivity for proteins binding to label-free antibodies. The importance of controlling nonspecific binding in biosensors using carbon nanotubes has been addressed.²² However, to the best of our knowledge, performance with real clinical samples has yet to be demonstrated.

Our research team has self-assembled 20–30 nm long terminally carboxylated single-wall carbon nanotubes (SWNT) into forests²³ standing in upright bundles on Nafion-iron oxide decorated conductive surfaces. The SWNTs forests were fully characterized using polarized Raman spectroscopy and atomic force microscopy, which confirmed the vertical orientation of the nanotubes in bundles of 20–100 nm diameter at coverage of >98% of the underlying solid substrate.²⁵ Efficient, direct electrical communication was achieved between the highly conductive nanotubes in these forests and peroxidase enzymes bioconjugated to their ends.^{24,25} We also attached antibodies to SWNT forest platforms to demonstrate proof-of-concept immunodetection of a small molecule, biotin,²⁶ and human serum albumin²⁵ in buffer solutions. Primary antibody on the SWNT sensor binds antigen in the sample, which in turn, binds a peroxidase-labeled antibody (Scheme 1A). Amperometric signals are developed by adding small amounts of hydrogen peroxide to a solution bathing the sensor to activate the peroxidase electrochemical cycle, and measuring the current for catalytic peroxide reduction while the sensor is under a constant voltage.^{25,26}

In this paper, we report a novel amplification strategy for SWNT immunosensors and applications to the detection of a cancer biomarker in real biomedical samples for the first time. While label-free strategies are attractive in that they eliminate the need for antibody labeling, herein we pursue a multi-label strategy that provides advantages of enhanced sensitivity and selectivity, the latter by virtue of requiring two specific binding events for detection.⁶ Greatly amplified sensitivity was achieved by using bioconjugates featuring horseradish peroxidase (HRP) labels and secondary antibodies (Ab₂) linked to multiwall carbon nanotubes (CNT) at high HRP/Ab₂ ratio to replace singly labeled secondary antibodies (Figure 1B). This resulted in a detection limit of 4 pg mL⁻¹ (100 amol mL⁻¹) for prostate specific antigen (PSA) in 10 μ L undiluted calf serum. PSA in human serum was measured with SWNT immunosensors with \pm 5% accuracy for human serum samples compared to a referee ELISA method. PSA in laser microdissected cancer cells from prostate tissue was measured more quantitatively than possible by the gold standard immunohistochemical method.

Experimental Section

Chemicals and Materials

Horseradish peroxidase (HRP, MW 44 000), lyophilized 99% bovine serum albumin (BSA) and Tween-20 were from Sigma/Aldrich. Monoclonal (Mouse) primary anti-human prostate specific antigen (PSA) antibody (clone no. CHYH1), tracer secondary anti-PSA antibody (clone no. CHYH2) with and without HRP conjugation, and PSA standard in calf serum were obtained from Anogen/Yes Biotech Lab, Ltd., antibodies are specific to t-PSA. Recombinant human PSA standard in phosphate buffered saline (PBS) were obtained by the methods described below. Human serum and prostate tissue samples from patients were obtained

anonymously from the National Cancer Institute. Single-walled carbon nanotubes (HiPco) were obtained from Carbon Nanotechnologies, Inc. Multiwalled carbon nanotubes were from Helix Inc. 2,2'-Azino-Bis(3-ethylbenzthiazoline-6-sulfonic acid) was from Sigma. Immunoreagents were dissolved in pH 7.0 phosphate saline (PBS) buffer (0.01 M in phosphate, 0.14 M NaCl, 2.7 mM KCl) unless otherwise noted. 1-(3-(dimethylamino)-propyl)-3-ethylcarbodiimide hydrochloride (EDC) and N-hydroxysulfosuccinimide (NHSS) were dissolved in water immediately before use.

Fabrication of SWNT Immunosensors

SWNT forests were assembled and characterized by AFM and Raman spectroscopy as reported previously.²⁵ Briefly, SWNTs were first carboxyl-functionalized and shortened by sonication in 3:1 HNO₃/H₂SO₄ for 4 h at 70 °C.²³ These dispersions were filtered, washed with water, dried, and dispersed in DMF. Abraded, ordinary basal plane pyrolytic graphite (PG) disks (A) 0.16 cm²) were prepared for forest assembly by forming a thin layer of Nafion and Fe (OH)_x on their surfaces.^{23,25} After immersion of these substrates into aged DMF dispersions of shortened SWNTs, vertically assemblies of SWNTs are formed (forests), which were then dried in a vacuum for 18 h.

For attachment of primary antibody, 30 μ L of freshly prepared 400 mM EDC and 100 mM NHSS in water were placed onto the SWNT forest electrodes, and washed off after 10 min. This was immediately followed by 3 h incubation at 37 °C with 20 μ L of 2 nmol mL⁻¹ (0.33 mg/mL) primary anti-PSA antibody (Ab₁) in pH 7.0 PBS buffer containing 0.05% Tween-20. The electrode was then washed with 0.05% Tween-20 and PBS buffer. The anti-PSA/SWNT electrode sensor constructed as described above was incubated for 1 h at 37 °C with 20 μ L of 2% BSA + 0.05% Tween-20, followed by washing with 0.05% Tween-20 and PBS buffer for 3 min. Washing steps used here and during PSA analysis were essential to block nonspecific binding (NSB), and omission of any of the washing steps deteriorated sensitivity.

Production of Recombinant PSA

HEK293T cells grown overnight (10 cm plates) were transfected with 1 μ g pSecTag2/PSA DNA (Invitrogen) using polyfect reagent (Qiagen). Transfected cells were grown initially for 24 h, and then again for a similar period in media without serum. Purification of epitope tagged (His-myc) containing PSA was done by first collecting condition media from the transfected cells, centrifuging to remove debris and incubating with equilibrated TALON resin (Invitrogen) for 20 min at room temperature to bind only His-containing PSA. After this step, resin was collected by centrifugation, washed, and then transferred to a 2 mL gravity-flow column. Resin in the column was washed again, and PSA eluted by passing elution buffer through the column, 500 μ L fractions were collected.

For quality assurance, 5 μ L of each fraction was analyzed by western blot, and probed for myc (epitope tag). Fractions with high levels of His-myc tagged-PSA were pooled and concentrated using Centricon YM30 from approximately 1 mL to 200 μ L. The total concentration of PSA was determined by resolving 5–10 μ L of the concentrated fraction on a SDS gel together with BSA standards, and scanned after staining with Coomassie blue. Using NIH Image software, only the band corresponding to the molecular weight (44 kDa) of the epitope tagged PSA was quantified against the BSA standards. Concentration was expressed in ng μ L⁻¹.

Laser Capture Microdissection (LCM)²⁷ of Prostate Tissue

Frozen tissue section slides were stained prior to LCM by briefly fixing tissue sections in 70% ethanol (30 s), followed by water washes, staining in Mayer's hematoxylin (30 s), rinsing in 70% ethanol, and dehydration with 95–100% ethanol and SAFECLEAR II (xylene substitute; Fisher Diagnostics, VA). The stained uncovered tissue sections were air-dried and viewed

through the microscope, and after locating the cells of interest, a CapSure LCM Cap (Molecular Devices Corporation) was placed over the target area and pulsed with laser to adhere cells to the cap. After sufficient cell capture, caps were transferred to a 0.5 mL sterile microfuge tube for immediate processing. For each sample, approximately 1000 cells were captured and subsequently processed for protein extraction. Briefly, 20 μ L T-PER tissue protein extraction buffer (Pierce) was placed in each tube with the enclosed caps, the tubes were inverted to ensure that the buffer was adequately dispersed to cover the surface of the caps and vortexed for 10 s, followed by incubation on ice for 10 min. The extraction solution was then recovered by centrifugation at 14 000 rpm for 2 min, then stored at -80°C until ready for analysis.

Preparation of the Ab₂-MWCNT-HRP Bioconjugates

MWCNTs were functionalized and shortened with 4–6 h probe sonication using a Fisher Sonic Dismembrator (Model 300) with a titanium microtip (15–338–41) inserted in the center of the cell and set at 60% power in 3:1 H₂SO₄/HNO₃ ($\sim 70^{\circ}\text{C}$). The resulting dispersion was washed repeatedly with water and filtered until pH was ~ 7 . The resulting functionalized, shortened MWCNTs were then dried under vacuum overnight. This procedure removes metallic and carbonaceous impurities and generates carboxylate groups on the shortened nanotubes.^{28,29} Subsequently, 1.5 mg of the functionalized MWCNTs were dispersed in 2 mL pH 7 PBS buffer and sonicated for 10 min to obtain a homogeneous dispersion, which indicated that the MWCNTs were well functionalized with hydrophilic carboxylate groups. This dispersion was then mixed with 1 mL of 400 mM EDC and 100 mM NHSS in pH 6.0 MES buffer and vortexed at room temperature for 15 min. The resulting mixture was centrifuged at 15 000 rpm for 5 min, and the supernatant was discarded. The buffer wash was repeated to remove excessive EDC and NHSS. Secondary anti-PSA antibody (Ab₂) at 0.005 mg/mL and HRP at 1 mg/mL were added to the mixture and stirred in a small vial overnight at room temperature (Scheme 2). The reaction mixture was then centrifuged at 15 000 rpm at 4°C for 10 min, and supernatant was removed. 1 mL PBS buffer was added to the solid conjugate remaining in the vial, mixed well, and centrifuged again at 15 000 rpm at 4°C for 10 min, and the supernatant was discarded. This step served to remove any free HRP and Ab₂ and was repeated 4 more times. 1 mL of 0.05% Tween-20/PBS buffer was added to the bioconjugate precipitate collected, vortexed to form an homogeneous dispersion, and stored in refrigerator at 4°C , and diluted by PBS/0.05% Tween-20 immediately before use. The bioconjugates were characterized by tapping mode AFM and enzyme activity assays as described in the text.

To avoid problems from slow precipitation of Ab₂-MWCNT-HRP bioconjugates, the well dispersed portion of the supernatant liquid was removed and diluted 10-fold immediately before use for immuno-sensing. Bioconjugate dispersions were stable for a week at 4°C as shown by reproducible signals for PSA standards.

Instrumentation

A CHI 660 electrochemical workstation was used for cyclic voltammetry and amperometry at ambient temperature ($22\pm 2^{\circ}\text{C}$) in a three-electrode cell. Amperometry was done at -0.3 V vs SCE with the SWNT working electrode rotated at 3000 rpm, as these conditions gave optimum sensitivity. A Nanoscope IV multimode atomic force microscope and a TA Instruments Q600 simultaneous differential scanning calorimeter-thermal gravimetric analyzer (DSC-TGA) were used for the characterization of Ab₂-CNT-HRP bioconjugates.

Immunosensor Detection of PSA

Optimized steps in the assay procedure were as follows:

1. The immunosensor, prepared and preincubated with 2% BSA + 0.05% Tween-20 as described above, was secured in an inverted position and incubated at 37°C for 1 h

15 min with a 10 μL drop of serum containing PSA, followed by washing with 0.05% Tween-20 in buffer and then PBS buffer for 1.5 min each.

2. Next, the inverted sensor was incubated with 10 μL of 4 pmol mL^{-1} HRP-labeled anti-PSA antibody ($\text{Ab}_2\text{-HRP}$) in buffer containing 2% BSA and 0.05% Tween-20 at 37 $^\circ\text{C}$ for 1 h 15 min, or 10 μL of $\text{Ab}_2\text{-CNT-HRP}$ bioconjugate (11 pmol mL^{-1} in HRP) in buffer containing 0.05% Tween-20 at 37 $^\circ\text{C}$ for 1 h 15 min, followed by washing in 0.05% Tween-20 and PBS buffer for 3 min.
3. The immunosensor was then placed in an electrochemical cell containing 10 mL pH 7.0 PBS buffer and 1 mM hydroquinone. Rotating disk amperometry at 3000 rpm was done at -0.3 V vs SCE. To develop the amperometric signals, H_2O_2 was injected to 0.4 mM when using $\text{Ab}_2\text{-HRP}$, and H_2O_2 was injected to 0.04 mM when using $\text{Ab}_2\text{-CNT-HRP}$.

Results

SWNT Immunosensor Using Conventional $\text{Ab}_2\text{-HRP}$

Prostate specific antigen (PSA) is a biomarker for prostate carcinoma, and is an established clinical tool for diagnosing and monitoring the disease.³⁰ We first analyzed undiluted calf serum containing different amounts of PSA with the SWNT immunosensors with anti-PSA attached (Figure 1A). Inhibition of nonspecific binding (NSB) was critical to achieve the best sensitivity and detection limits. Thus, we developed a highly effective blocking procedure utilizing competitive binding of bovine serum albumin (BSA) and the detergent Tween-20, and also optimized the concentration of tracer secondary anti-PSA antibody ($\text{Ab}_2\text{-HRP}$) (see Experimental Section). Before exposure to the sample, immunosensors were incubated for 1 h with 20 μL 2% BSA + 0.05% Tween-20, then washed with 0.05% Tween-20 in buffer. For measurements, 10 μL undiluted new born calf serum containing PSA was incubated on the inverted sensor surface, blocking buffer was used to wash, then the sensor was incubated with 10 μL HRP-labeled secondary anti-PSA. The washed immunosensor was then placed into an electrochemical cell containing the mediator hydroquinone in buffer, and hydrogen peroxide was injected for signal development (Figure 1A).

The steady state current increased linearly (Figure 1B) with PSA concentration over the range 0.4–40 ng mL^{-1} , encompassing the 4–10 ng mL^{-1} prostate cancer prediction range for human serum. Excellent device-to-device reproducibility is illustrated by the small error bars, and sensitivity of 10.6 nA-mL ng^{-1} (Figure 1B) was achieved. The detection limit of 0.4 ng mL^{-1} as the zero PSA control signal plus three-times the control noise level (Figure 1Aa) was similar to that obtained for PSA in buffers (not shown). Results indicate that using BSA and detergent for NSB blocking, and optimizing the concentration of $\text{Ab}_2\text{-HRP}$ is very effective to minimize NSB in serum.

Control experiment (a) in Figure 1A represents a SWNT immunosensor taken through the full procedure without exposure to PSA, and the response reflects the sum of residual NSB and direct reduction of hydrogen peroxide. Other controls are immunosensors with no nanotubes on bare PG (b) and on the Nafion-iron oxide-coated PG underlayer used for SWNT forests (c), then exposed to the full assay procedure using 40 ng mL^{-1} PSA. The response in each case was 3-fold smaller than that of the full SWNT immunosensor at the same concentration of PSA, and only a little larger than that of control (a) with no PSA. The significant increase for the SWNT immunosensor response compared to these latter controls show that the presence of the vertical nanotube forest provides a significant amplification of the amperometric signal.

Ab₂-CNT-HRP Bioconjugates

A biomaterial bearing multiple HRP labels attached to nanotube segments was developed for multi-label amplification^{31,32} to enhance sensitivity. Our approach was to link HRP and Ab₂ to carboxylated multiwall carbon nanotubes (CNT) using the EDC/NHSS protocol²⁵ with a reaction mixture having a 200/1 HRP/Ab₂ molar ratio (Scheme 2). This biomaterial was made to replace the conventional Ab₂-HRP complex. Atomic force microscopy (AFM) images of sonicated, carboxylated nanotubes revealed heights of 20~25 nm and predominate lengths of 0.5–1.5 μm (with some <0.5 μm), compared to pristine CNTs with diameters of 10–30 nm and lengths of 0.5 to 40 μm before sonication (Figure 2A).

Ab₂ and HRP were covalently linked to carboxylated CNTs, by a two-step process. Carboxylic acid groups on CNTs were first activated using EDC and NHSS,³³ which were then removed, and the CNT material was reacted with amine residues on the proteins. This process avoids protein cross-linking, which we found to form bundles of the Ab₂-CNT-HRP bioconjugates that may deteriorate detection performance.

Figure 2 shows AFM images of isolated, carboxylated CNTs before and after bioconjugation with HRP and Ab₂. Size analysis showed that the image before bioconjugation had an average height of 24.5 nm, whereas the images of nanotubes with HRP and Ab₂ attached had average heights of 34.2 nm. The 10 nm increase in height for the bioconjugate nanotubes is consistent with the average thickness of a monolayer of the major coating component HRP (4.0 \times 6.7 \times 11.7 nm, Brookhaven Protein Database) on the 25 nm nanotubes. Furthermore, after protein binding, globular shapes suggestive of protein aggregates appeared on the side walls of the nanotubes.

To determine the amount of active HRP per unit weight of CNT and per nanotube length, the HRP-CNT-Ab₂ dispersion was reacted with HRP substrate 2,2'-azino-bis-(3-ethylbenzthiazoline-6-sulfonic acid) (ABTS)³⁴ and H₂O₂. The reaction produces a soluble product with characteristic optical absorbance peak at 405 nm. This was compared to a standard curve constructed with underivatized HRP, after subtracting the background absorbance of an equivalent dispersion of underivatized CNTs. The concentration of active HRP in the stock HRP-CNT-Ab₂ dispersion was determined by these enzyme activity experiments to be 4.75 $\mu\text{g mL}^{-1}$. Simultaneous differential scanning calorimeter-thermal gravimetric analysis was used to remove HRP and Ab₂ from the bioconjugate by heating to 600 °C and this showed the total mass of CNT to be 0.297 mg mL⁻¹ of dispersion. From these data, the amount of active HRP was found to be 340 pmol HRP/mg CNT, or 108 pmol HRP mL⁻¹ of dispersion. Using a model for the nanotubes with 25 nm average diameter, the total number of CNTs of the estimated 1 μm avg. length was 14×10^{11} , and number of active HRP per CNT was estimated at ~87 active HRP per CNT. Thus, for the 1 μm average nanotube length, and one bioconjugate nanotube bound per antigen, we estimate ~90 catalytic labels per binding event on immunosensor surfaces. Initial reactant concentrations in making the bioconjugates suggest ~0.5 Ab₂ per 1 μm of CNT. Thus, some nanotubes may not have any Ab₂, but they will only contribute to NSB. Increasing Ab₂ in the bioconjugate preparation did not improve sensitivity of detection limit, and it introduced irreproducibility.

Similar NSB blocking protocols as summarized for Ab₂-HRP were followed when using the Ab₂-CNT-HRP bioconjugate (Scheme 1B) to measure response of the SWNT immunosensor to PSA. Optimization of bioconjugate concentration, a major factor in minimizing NSB, was done by evaluating the performance of dilutions of the stock Ab₂-CNT-HRP using 0.05% Tween-20. A 10-fold dilution to 11 pmol HRP mL⁻¹ gave the best detection limit. BSA was not used in the dilution as it was found to deteriorate the detection limit.

Figure 3A shows the amperometric detection of PSA in undiluted calf serum using the Ab₂-CNT-HRP conjugate with the SWNT immunosensors. Signal intensity was greatly improved compared to using the conventional Ab₂-HRP (cf. Figure 1A). Sensitivity as the slope of the calibration graph (Figure 3B) was 8430 nA·mL ng⁻¹, ~800 times higher than with Ab₂-HRP. Improved signal intensity led to a measured detection limit as 3 times the average noise above the zero PSA control of 4 pg mL⁻¹ in a 10 μL sample, for a mass detection limit of 40 fg. This is at least an order of magnitude better than any commercial PSA assay, for which mass detection limits are ≥700 fg. Control experiments showed that the signal from immunosensors based on bare PG or PG covered with Nafion-iron oxide underlayer is still 2.5 times smaller than SWNT immunosensor, again showing the advantage of SWNT forests in the immunosensor design. Comparison of the zero PSA control with the current from direct reduction of H₂O₂ suggested that residual NSB of the Ab₂-CNT-HRP bioconjugate is controlling the detection limit.

Measurement of PSA in Human Serum

Serum samples from cancer patients and cancer-free subjects were used to assess the accuracy of the immunosensor for real biomedical samples. Serum PSA within 4–10 ng mL⁻¹ is the “diagnostic gray zone”, which predicts that the patient has significant probability of prostate carcinoma.³⁵ SWNT immunosensors were used with the conventional Ab₂-HRP, which gave a linear response in this PSA concentration range (Figure 1B). Five clinically acquired human serum samples with varying PSA content were tested, and results are shown along with PSA standards in calf serum at comparable levels (Figure 4A). To evaluate the accuracy of using calf serum for the standards, standard addition, which minimizes errors from matrix effects, was done by adding three aliquots of PSA serum standard and extrapolating to the *x*-axis (Supporting Information, Figure S1). Samples were also analyzed by a standard ELISA method.

Comparison of immunosensor results with ELISA assays resulted in excellent correlations, as shown by the linear relationships in Figure 4B. Correlation coefficients for both direct and standard addition immunosensor results with ELISA were >0.999, and the slopes of the correlation graphs were close to one. The average accuracy of the immunosensor determination was (5% compared to ELISA. These results confirmed the validity of using undiluted calf serum in standards for SWNT immunosensor determination of PSA in human serum.

Amplified Detection of PSA in Human Prostate Cancer Biopsies

PSA is expressed in normal prostate tissue as well as in other carcinomas. While the present system of scoring tissue protein expression semiquantitatively by immunohistochemistry has been very useful,^{36,37} the potential to measure protein expression more precisely in tissue samples may improve diagnosis and prognosis of disease processes occurring in tissue, as well as detect therapeutic targets. To explore this potential with the SWNT immunosensors using the Ab₂-CNT-HRP bioconjugates, we tested prostate tissue lysates (see the Experimental Section). As seen in Figure 5, PSA was easily measured in approximately 1000 cancer cells. The signal from tumor cells was 2–6 times larger than the control signal for no cancer cells. Results obtained by comparison to PSA standards in calf serum were as follows: sample 1, 90 attogram (ag) PSA/cell; sample 2, 51 ag PSA/cell; and sample 3, 830 ag PSA/cell. Using the “gold standard” histological tissue stain scoring system³⁶ on the standard scoring scale of 0–3+, all of the tissue samples scored 3+ for PSA. Results show that differences in PSA concentration can be detected with the SWNT immunosensors for tissue samples that cannot be distinguished by the immunohistochemistry staining method.

Discussion

Results described above show that SWNT immunosensors can accurately detect cancer biomarkers in complex biological samples with very high sensitivity (Figure 3) and selectivity (Figures 4 and 5). Further, the immunosensors have a very good reproducibility, as demonstrated by device-to-device standard deviations with both Ab₂-CNT-HRP bioconjugates and conventional single-label HRP-Ab₂. The best sensitivity is obtained using the Ab₂-CNT-HRP bioconjugates with high enzyme label/ Ab₂ ratios for signal amplification. The success of this novel signal amplification strategy also depends on minimizing the nonspecific binding (NSB) of the secondary antibody material, which commonly controls the detection limit of sandwich immunoassays.^{6,13} NSB was effectively controlled by using BSA and Tween-20 in blocking buffers, providing sensitivity to PSA at concentrations as low as 4 pg mL⁻¹ in only 10 μ L of undiluted calf serum (Figure 3A), which contains $\sim 10^{10}$ times more unrelated protein than the cancer biomarker being detected.³⁸ Furthermore, SWNT immunosensors were capable of sensitive quantitative measurement of PSA in 1000 prostate cancer cells (Figure 5), in tissue samples that cannot be distinguished from one another with the best immunostaining methodologies. In addition, good accuracy was demonstrated by excellent correlation of SWNT immunosensor results obtained in two different ways for PSA in human serum samples with standard ELISA results on the same samples (Figure 4).

SWNT immunosensors using the Ab₂-CNT-HRP bioconjugates gave superior mass sensitivity to all commercial PSA immunoassays currently available. The immunosensors require 10 times less sample than these methods, and had a mass detection limit 10–100 times better than commercial assays such as ELISA, Elecsys, IMX, and Tandem-R.¹⁰⁻¹³ A recent study²¹ reported elegant Si-nanowire nanotransistor devices encased in a microfluidics device that achieved detection of 0.9 pg mL⁻¹ PSA in undiluted monkey serum using conductance changes associated with binding of PSA to anti-PSA antibodies on the nanowires. This is the very best PSA detection limit reported thus far for an immunological device that does not require PCR amplification³⁹ and complex post-binding manipulations. From the reported flow rate (150 μ L/hr) and the time to steady-state (~ 1200 s), 50 μ L of sample was required to achieve the reported nanotransistor detection limit in serum.²¹ The actual mass detection limit of the Si nanotransistor (45 fg) in serum is slightly larger than what we found with SWNT immunosensors (40 fg), although the difference is probably not statistically significant. An advantage of our approach is that SWNT forest fabrication is simple, and requires only room temperature, solution-based fabrication steps.

The high sensitivity of the SWNT immunosensors using the Ab₂-CNT-HRP bioconjugates relies upon three types of amplification: (a) the labeling protocol allows several hundred labels per binding event provided by using Ab₂-CNT-HRP bioconjugates in place of conventional Ab₂-HRP; (b) SWNT forest properties including excellent conductivity and high surface area that provides a high density of primary antibodies,²⁵ and (c) the catalytic nature of the enzyme label, in which HRP is activated by hydrogen peroxide to a ferryl-oxo form of the enzyme that is electrochemically reduced in a catalytic cycle.⁴⁰ It is possible that sensitivity could be improved further by optimizing Ab₂-CNT-HRP properties, and by further decreasing NSB of these bioconjugates. Moreover, preliminary studies of SWNT arrays in our laboratories suggest an excellent potential for array fabrication leading to real time multiplexed cancer biomarker detection, an exciting possibility that we are currently exploring. Immobilization of enzyme labels at the sensing element as in our approach is ideal for arrays as it prohibits electrochemical crosstalk between array elements, which can occur with enzymes producing a soluble electroactive product.^{41,42}

In conclusion, we have demonstrated highly sensitive and selective electrochemical detection of a protein cancer biomarker with SWNT immunosensors, as exemplified by the measurement

of PSA in complex biomedical samples such as human serum and tissue lysates. The detection limit of 4 pg mL^{-1} surpasses detection limits for PSA by commercial immunoassay methods, as well as most recently reported experimental biosensor approaches. SWNT immunosensors can be adapted easily for the detection of other relevant biomarkers and have the potential for fabrication into arrays to facilitate multiplexed detection. We believe that such devices will evolve toward a very promising future for reliable point-of-care diagnostics of cancer and other diseases, and as tools for intra-operation pathological testing, proteomics, and systems biology.

Supplementary Material

Refer to Web version on PubMed Central for supplementary material.

Acknowledgment

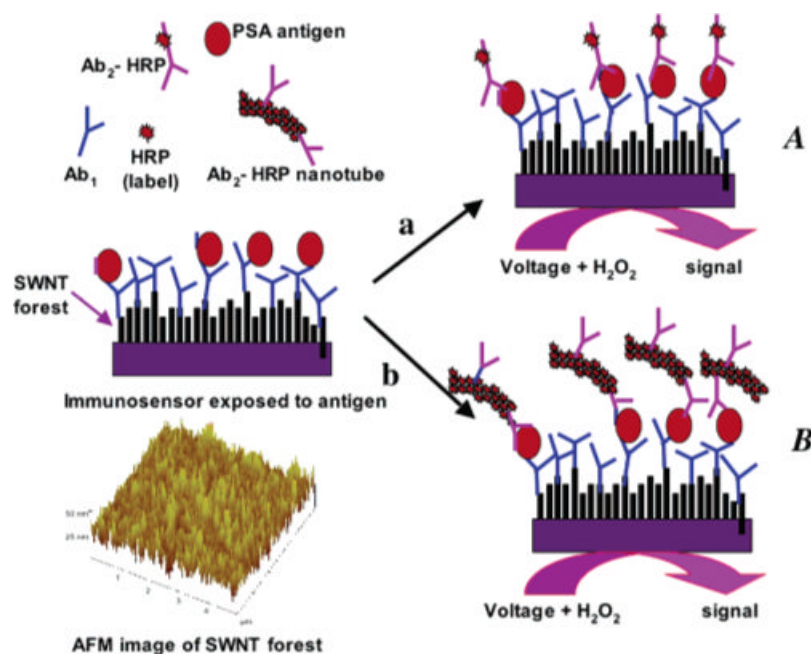
Work at the University of Connecticut was supported by U.S. Army Research Office (ARO) via grant DAAD-02-1-0381 and in part by PHS grant ES013557 from NIH. Partial support was also provided by the intramural program of the National Institute of Dental and Craniofacial Research. Patient tissue samples were obtained from Institutional Review Board (IRB)-approved clinical protocols. We thank Michael R. Emmert-Buck, Rodrigo F. Chuaqui, and Marston W. Linehan of the Center for Cancer Research, National Cancer Institute, and Alfredo Velasco (Departments of Urology and Pathology, Catholic University, Santiago, Chile) for their support and help.

Supporting Information Available: An Additional figure illustrating standard addition immunosensor determination of PSA in human tissue samples, and a table comparing values of PSA found for immunosensor methods and ELISA. This material is available free of charge via the Internet at <http://pubs.acs.org>. See any current masthead page for ordering information and Web access instructions.

References

1. Kitano H. *Science* 2002;295:1662–1664. [PubMed: 11872829]
2. Figeys D. *Anal. Chem* 2003;75:2891–2905. [PubMed: 12945794]
3. Sander C. *Science* 2000;287:1977–1978. [PubMed: 10755952]
4. Srinivas PR, Kramer BS, Srivastava S. *Lancet Oncol* 2001;2:698–704. [PubMed: 11902541]
5. Stevens EV, Liotta LA, Kohn EC. *Int. J. Gynecol. Cancer* 2003;13:133–139. [PubMed: 14656269]
6. Wilson DS, Nock S. *Angew. Chem., Int. Ed* 2003;42:494–500.
7. Xiao Z, Prieto D, Conrads TP, Veenstra TD, Issaq HJ. *Mol. Cell. Endocrinol* 2005;230:95–106. [PubMed: 15664456]
8. Weston AD, Hood L. *J. Proteome Res* 2004;3:179–196. [PubMed: 15113093]
9. Wagner PD, Verma M, Srivastava S. *Ann. N. Y. Acad. Sci* 2004;1022:9–16. [PubMed: 15251933]
10. Vessella R, Noteboom J, Lange P. *Clin. Chem* 1992;38:2044–2054. [PubMed: 1382897]
11. Woodrums D, French C, Hill T, Roman S, Shamel L. *Clin. Chem* 1997;43:1203–1208. [PubMed: 9216457]
12. Butch A, Crary D, Yee M. *Clin. Biochem* 2002;35:143–145. [PubMed: 11983350]
13. Ward AM, Catto JWF, Hamdy FC. *Ann. Clin. Biochem* 2001;38:633–651. [PubMed: 11732646]
14. Chou SF, Hsu WL, Hwang JM, Chen CY. *Biosens., Bioelectron* 2004;19:1999–2005.
15. Haes AJ, Hall WP, Chang L, Klein WL, Van Duyne RP. *Nano. Lett* 2004;4:1029–1034.
16. Alivisatos P. *Nature Biotech* 2004;22:47–52.
17. Wang Z, Lee J, Cossins AR, Brust M. *Anal. Chem* 2005;77:5770–5774. [PubMed: 16131095]
18. Wu G, Datar R, Hansen K, Thundat T, Cote R, Majumdar A. *Nature Biotech* 2001;19:856–860.
19. Chen RJ, Choi HC, Bangsaruntip S, Yenilmez E, Tang X, Wang Q, Chang Y-L, Dai H. *J. Am. Chem. Soc* 2004;126:1563–1568. [PubMed: 14759216]
20. Li C, Curreli M, Lin H, Lei B, Ishikawa FN, Datar R, Cote R, Thompson M, Zhou C. *J. Am. Chem. Soc* 2005;127:12484–12485. [PubMed: 16144384]
21. Zheng G, Patolsky F, Cui Y, Wang W, Lieber C. *Nature Biotechnol* 2005;23:1294–1301. [PubMed: 16170313]

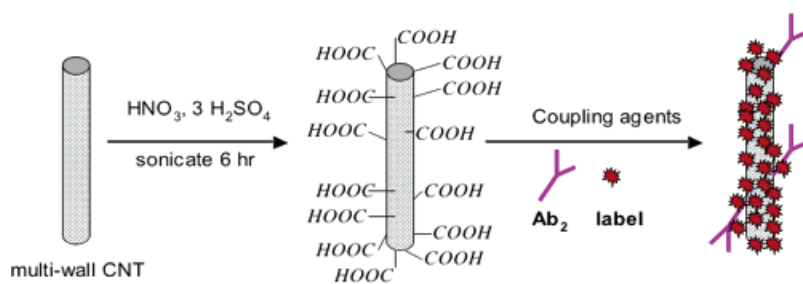
22. a Shim M, Kam NWS, Chen RJ, Li Y, Dai H. *Nano. Lett* 2002;2:285–288. b Chen RJ, Bangsaruntip S, Drouvalakis KA, Kam NWS, Shim M, Li Y, Kim W, Utz PJ, Dai H. *Pro. Natl. Acad. Sci. U.S.A* 2003;100:4984–4989.
23. Chattopadhyay D, Galeska I, Papadimitrakopoulos F. *J. Am. Chem. Soc* 2001;123:9451–9452. [PubMed: 11562232]
24. Yu X, Chattopadhyay D, Galeska I, Papadimitrakopoulos F, Rusling JF. *Electrochem. Comm* 2003;5:408–411.
25. Yu X, Kim S, Papadimitrakopoulos F, Rusling JF. *Mol. Biosys* 2005;1:70–78.
26. O'Connor M, Kim SN, Killard AJ, Forster RJ, Smyth MR, Papadimitrakopoulos F, Rusling JF. *Analyst* 2004;129:1176–1180. [PubMed: 15565214]
27. Emmert-Buck MR, Bonner RF, Smith PD, Chauqui RF, Zhuang Z, Goldstein SR, Weiss RA, Liotta LA. *Science* 1996;274:998–1001. [PubMed: 8875945]
28. Liu J, Rinzler AG, Dai HJ, Hafner JH, Bradley RK, Boul PJ, Lu A, Iverson T, Shelimov K, Huffman CB, Rodriguez-Macias F, Shon Y-S, Lee TR, Colbert DT, Smalley RE. *Science* 1998;280:1253–1256. [PubMed: 9596576]
29. Liu J, Casavant MJ, Cox M, Walters DA, Boul P, Lu W, Rimberg AJ, Smith KA, Colbert DT, Smalley RE. *Chem. Phys. Lett* 1999;303:125–129.
30. Chu TM. *J. Clin. Lab. Anal* 1994;8:323–326. [PubMed: 7528795]
31. Wang J. *Small* 2005;1:1036–1043. [PubMed: 17193390]
32. Munge B, Liu G, Collins J, Wang J. *Anal. Chem* 2005;77:4662–4666. [PubMed: 16013886]
33. Sehgal D, Vijay IK. *Anal. Biochem* 1994;218:87–91. [PubMed: 8053572]
34. Matsuda H, Tanaka H, Blas BL, Nosenas JS, Tokawa T, Ohsawa S. *Jpn. J. Exp Med* 1984;54:131–138. [PubMed: 6542945]
35. Blijenberg BG, Kranse R, Eman I, Schroder FH. *Eur. J. Clin. Chem. Clin. Biochem* 1996;34:817–821. [PubMed: 8933105]
36. Gannot G, Gillespie JW, Chuaqui RF, Tangrea MA, Linehan WM, Emmert-Buck MR. *J. Histochem. Cytochem* 2005;53:177–185. [PubMed: 15684330]
37. Simone NL, Remaley AT, Charboneau L, Petricoin EF, Glickman JW, Emmert-Buck MR, Fleisher TA, Liotta LA. *Am. J. Pathol* 2000;156:445–452. [PubMed: 10666374]
38. Alalya A, Al-Mohanna M, Linder S. *J. Proteome Res* 2005;4:1213–1222. [PubMed: 16083271]
39. Nam JM, Thaxton CS, Mirkin CA. *Science* 2003;301:1884–1886. [PubMed: 14512622]
40. Ruzgas, T.; Lindgren, A.; Gorton, L.; Hecht, H-J.; Reichelt, J.; Bilitewski, U. *Electroanalytical Methods for Biological Materials*. Chambers, JQ.; Bratjer-Toth, A., editors. Marcel Dekker; New York: 2002. p. 233–254.
41. Kojima K, Hiratsuka A, Suzuki H, Yano K, Ikebukuro K, Karube I. *Anal. Chem* 2003;75:1116–1122. [PubMed: 12641231]
42. Wilson MS. *Anal. Chem* 2005;77:1496–1502. [PubMed: 15732936]



Scheme 1.

Illustration of Detection Principles of SWNT Immunosenors^a

^a On the bottom left is a tapping mode atomic force microscope image of a SWNT forest that serves as the immunosensor platform. Above this on the left is a cartoon of a SWNT immunosensor that has been equilibrated with an antigen, along with the biomaterials used for fabrication (HRP is the enzyme label). Picture **A** on the right shows the immunosensor after treating with a conventional HRP-Ab₂ providing one label per binding event. Picture **B** on the right shows the immunosensor after treating with HRP-CNT-Ab₂ to obtain amplification by providing numerous enzyme labels per binding event. The final detection step involves immersing the immunosensor after secondary antibody attachment into a buffer containing mediator in an electrochemical cell, applying voltage, and injecting a small amount of hydrogen peroxide.



Scheme 2.
Preparation of Ab_2 -MWCNT-HRP Bioconjugates

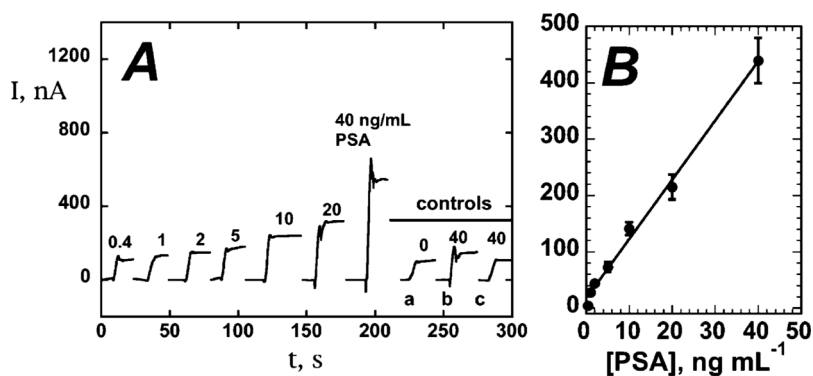


Figure 1.

Amperometric response for SWNT immunosensors incubated with PSA in 10 μ L undiluted newborn calf serum for 1.25 h, then conventional anti-PSA-HRP in 2% BSA and 0.05% Tween-20 for 1.25 h, (A) showing current at -0.3 V and 3000 rpm after placing electrodes in buffer containing 1 mM hydroquinone mediator, then injecting H_2O_2 to 0.4 mM to develop the signal. Controls shown on right with PSA concentrations: (a) full SWNT immunosensor omitting addition of PSA, (b) immunosensor built on bare PG surface at 40 ng mL⁻¹ PSA, (c) immunosensor built on Nafion-iron oxide-coated PG surface at 40 ng mL⁻¹ PSA; and (B) influence of PSA concentration on steady-state amperometric current for SWNT immunosensor using anti-PSA-HRP. Error bars in part B represent device-to-device standard deviations ($n = 3$).

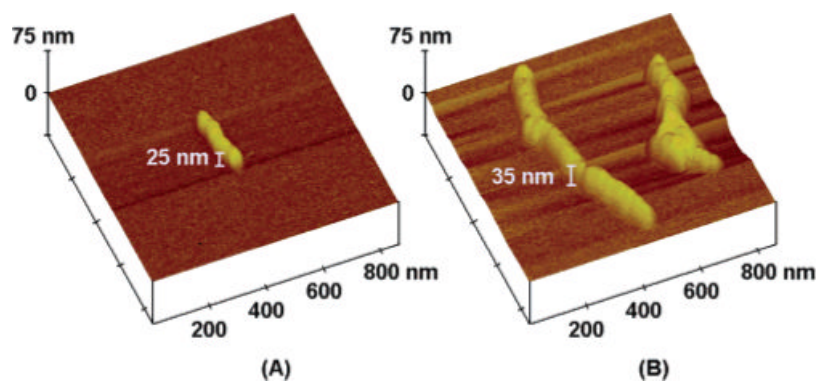


Figure 2. Tapping mode AFM images of sonicated, surface carboxylated MWCNTs isolated on smooth freshly cleaved mica surfaces (A) not derivatized with protein; and (B) derivatized as Ab₂-CNT-HRP bioconjugate.

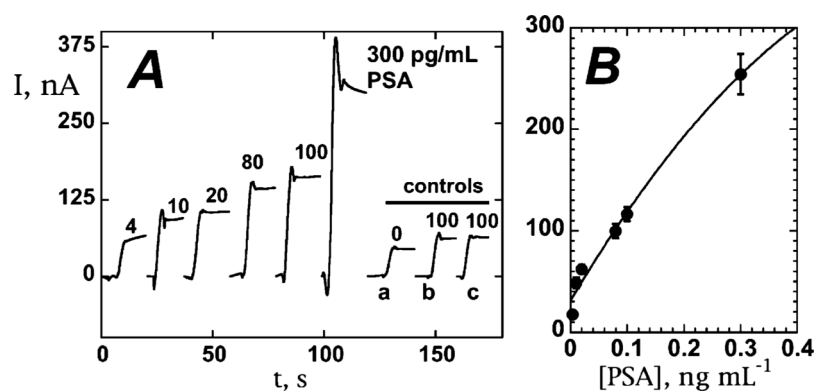


Figure 3.

Amperometric response for SWNT immunosensors incubated with PSA (concentration in pg mL⁻¹ labeled on curves) in 10 μ L undiluted newborn calf serum for 1.25 h: (A) current at -0.3 V and 3000 rpm using the Ab₂-CNT-HRP bioconjugate (11 pmol mL⁻¹ in HRP). Controls shown on right with PSA concentrations: (a) full SWNT immunosensor omitting addition of PSA, (b) immunosensor built on bare PG surface for 100 pg mL⁻¹ PSA, (c) immunosensor built on Nafion-iron oxide-coated PG electrode for 100 pg mL⁻¹ PSA. (B) Influence of PSA concentration on steady-state current for immunosensor using Ab₂-CNT-HRP bioconjugate. Error bars in part B represent device-to-device standard deviations ($n = 3$).

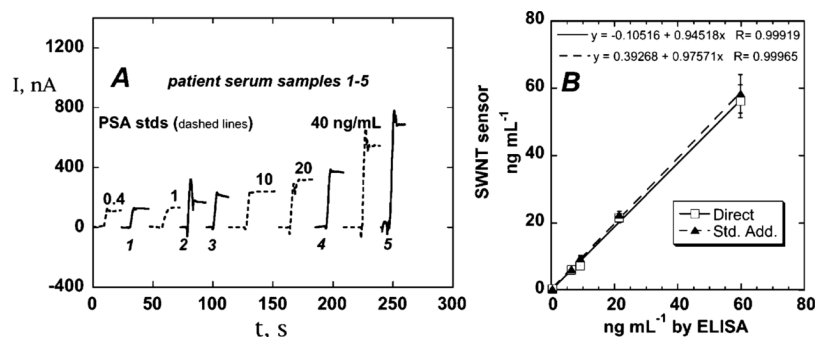


Figure 4.

Amperometric current at -0.3 V and 3000 rpm for human serum samples and PSA standards in calf serum (ng mL^{-1} labeled on curves, dashed lines). Immunosensors were incubated with $10 \mu\text{L}$ serum for 1.25 h followed by $10 \mu\text{L}$ 4 pmol mL^{-1} anti-PSA-HRP in 2% BSA and 0.05% Tween-20 for 1.25 h: (A) current after placing electrodes in buffer containing 1 mM hydroquinone mediator, then injecting H_2O_2 to 0.4 mM. Dashed lines are standards in calf serum; solid lines are human serum samples; (B) Correlations of SWNT immunosensor results for human serum samples found by using direct comparison to a calibration curve (\square) and by standard addition (\blacktriangle) against results from ELISA determination ($\text{RSD} \pm 10\%$) for the same samples. Equations shown were found by linear regression.

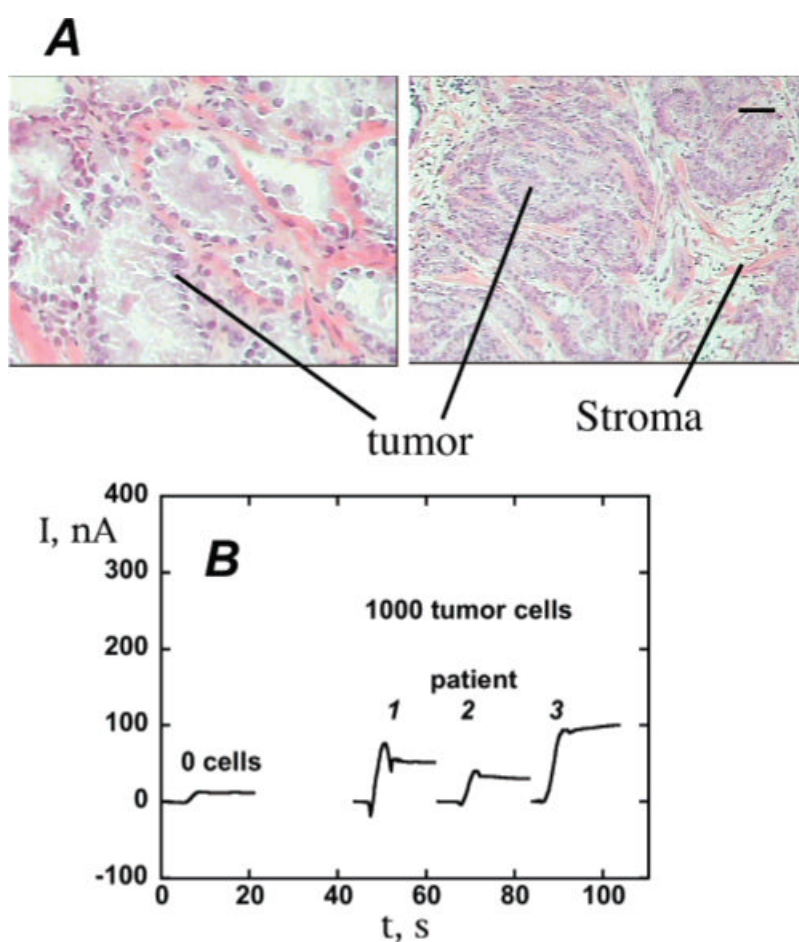


Figure 5.

Measurement of PSA in prostate cancer cells: (A) Micrograph of representative prostate cancer biopsy stained with haematoxylin and eosin to reveal areas of tumor and stromal cells (scale bar at upper right is 100 microns). Cells were subsequently procured by laser microdissection and processed for PSA detection by SWNT immunosensors. Nonmalignant normal cells (not shown) were processed similarly. (B) Amperometric current -0.3 V and 3000 rpm in which SWNT immunosensors were incubated with prostate tissue lysates (~ 1000 cells) in $10\ \mu\text{L}$ P-TER buffer for 1.25 h followed by $10\ \mu\text{L}$ anti-PSA-CNT-HRP bioconjugate ($11\ \text{pmol mL}^{-1}$ in HRP) in 0.05% Tween-20 for 1.25 h.